Published OnlineFirst February 1, 2011; DOI: 10.1158/0008-5472.CAN-10-1733

Cancer Research

Agonist Anti-CD137 mAb Act on Tumor Endothelial Cells to Enhance Recruitment of Activated T Lymphocytes

Asís Palazón[1], Alvaro Teijeira[1], Iván Martínez-Forero[1], Sandra Hervás-Stubbs[1], Carmen Roncal[1], Iván Peñuelas[1], Juan Dubrot[1], Aizea Morales-Kastresana[1], José Luis Pérez-Gracia[1], M. Carmen Ochoa[1], Laura Ochoa-Callejero[2], Alfredo Martínez[2], Alfonso Luque[3], Joseph Dinchuk[4], Ana Rouzaut[1], Maria Jure-Kunkel[4], and Ignacio Melero[1]

Abstract

Agonist monoclonal antibodies (mAb) to the immune costimulatory molecule CD137, also known as 4-1BB, are presently in clinical trials for cancer treatment on the basis of their costimulatory effects on primed T cells and perhaps other cells of the immune system. Here we provide evidence that CD137 is selectively expressed on the surface of tumor endothelial cells. Hypoxia upregulated CD137 on murine endothelial cells. Treatment of tumor-bearing immunocompromised *Rag*$^{-/-}$ mice with agonist CD137 mAb did not elicit any measurable antiangiogenic effects. In contrast, agonist mAb stimulated tumor endothelial cells, increasing cell surface expression of the adhesion molecules intercellular adhesion molecule (ICAM)-1, vascular cell adhesion molecule (VCAM)-1, and E-selectin. When adoptively transferred into mice, activated T lymphocytes derived from CD137-deficient animals entered more avidly into tumor tissue after treatment with agonist mAb. This effect could be neutralized with anti–ICAM-1 and anti–VCAM-1 blocking antibodies. Thus, stimulation of CD137 not only enhanced T-cell activation but also augmented their trafficking into malignant tissue, through direct actions on the blood vessels that irrigate the tumor. Our findings identify an additional mechanism of action that can explain the immunotherapeutic effects of agonist CD137 antibodies. *Cancer Res; 71(3); 801–11. ©2011 AACR.*

Introduction

CD137 (4-1BB, TNFRSF9) is a surface glycoprotein involved in T-cell costimulation (1–3). It was first described as a molecule selectively expressed on activated, but not resting, T lymphocytes (1–3). More recently, its expression has been documented on activated natural killer (NK) cells (4), dendritic cells (5), and other leukocytes such as mast cells (6), activated B lymphocytes, (7) and bone marrow myeloid precursors (8). The stimulatory effects of this receptor are elicited on interaction with the only described cognate ligand (CD137L, 41BBL, or TNFSF9) whose expression seems to be restricted to activated antigen presenting cells such as dendritic cells, macrophages, and B cells (1).

Authors' Affiliations: [1]CIMA and CUN University of Navarra, Pamplona, Spain; [2]Oncology Area, Center for Biomedical Research of La Rioja (CIBIR), Logroño, Spain; [3]Department of Regenerative Cardiology, Fundación Centro Nacional de Investigaciones Cardiovasculares Carlos III, Madrid, Spain; and [4]Research and Development, Bristol Myers-Squibb, Princeton, New Jersey

Note: Supplementary data for this article are available at Cancer Research Online (http://cancerres.aacrjournals.org/).

I. Melero and M. Jure-Kunkel will equally share credit for senior authorship.

Corresponding Author: Ignacio Melero, CIMA and Clinica Universitaria, Universidad de Navarra, Av. Pio XII, 55, 31008 Pamplona, Spain. Phone: 0034-9481-94700; Fax: 0034-9481-94717. E-mail: imelero@unav.es

doi: 10.1158/0008-5472.CAN-10-1733

While investigating genes whose expression was related to oncological angiogenesis, as opposed to the angiogenesis that occurs in nonmalignant tissue regeneration, it was found that mouse CD137 RNA probes were a selective marker of tumor related angiogenesis (9). Indeed, immunohistochemical evidence for CD137 expression on human malignant tumor capillaries had been previously obtained by the group of H. Schwarz (10). Moreover, evidence of expression of CD137 on the endothelial lining of atherosclerotic lesions in mice has been published (11).

Agonist monoclonal antibodies (mAb) directed to anti-CD137 or multivalent RNA aptamers binding CD137 (12) have been shown to therapeutically enhance antitumor CD8 T-cell–mediated immunity in mice (3, 13–15). Interestingly, treatment with agonist anti-CD137 mAb can overcome tumor antigen tolerance (16) in a number of models and more importantly, can be successfully combined with both other immunotherapeutic strategies (17–20) and conventional immune-unrelated treatment approaches (17, 21). Some of those combinations attain extraordinary therapeutic activity in mouse models (22). For these reasons anti-human CD137 agonist mAb are undergoing phase I/phase II clinical trials (17). Paradoxically, similar antibody agents ameliorate autoimmune model diseases in mice (23–25) mainly because of interfering with autoreactive CD4 T cells (23, 24, 26). The only described inflammatory complication in mice treated with agonist anti-CD137 mAb are moderate liver infiltrates in which polyclonal CD8 T cells predominate (27, 28).

Published OnlineFirst February 1, 2011; DOI: 10.1158/0008-5472.CAN-10-1733

The mechanism of action has been interpreted in the sense that a stronger CD8 T-cell–mediated immune response is artificially costimulated in treated animals (3, 13, 29). Direct stimulation of the CD137 receptor on T cells is definitely involved in the immunotherapeutic effects, but the interaction of the agonist antibodies with CD137 expressed on the surface of activated NK cells (15, 30) and dendritic cells (5) can also be of importance (3).

If CD137 were expressed at the protein level on tumor endothelial cells, treatment with anti-CD137 mAb could signal into the vascular cells. We hypothesized that if CD137 signaled in the same way as in T cells via TNF receptor associated factor (TRAF) adaptors (1, 31, 32) toward NF-κB (31, 32), proinflammatory molecules could be induced. Among them, receptors that would increase T-cell homing to tumors, such as intercellular adhesion molecule (ICAM)-1, vascular cell adhesion molecule (VCAM)-1, and E-selectin, were postulated to be involved (33).

Our experiments show that adoptively transferred activated CD137-deficient T cells enter more avidly into tumor lesions as a result of enhanced expression of homing receptors on endothelial cells that have received direct stimulation via their surface CD137.

Material and Methods

Mice and cell lines

BALB/c wild-type (WT) mice (5–6 weeks old) were purchased from Harlan Laboratories. *Rag*$^{-/-}$ mice (BALB/c and C57BL/6) and MMTV-neuT mice (34) were purchased from the Jackson Laboratory and bred in our animal facility under specific pathogen-free conditions. CD137 knockout mice were generated at Lexicon Genetics. To generate CD137$^{-/-}$ mice, 129/Sv-derived embryonic stem (ES) cells (Lex1) were electroporated with a targeting construct that replaced the entire coding region of CD137 (exons 2–5) with a lacZneo fusion cassette (Supplementary Fig. S2). ES cells that survived neomycin selection (300 μg/mL) were amplified and split into several aliquots. From several hundred ES cell clones, 6 clones were identified that had the proper recombination events at the 5′ (internal probe) and 3′ ends (external probe; Supplementary Fig. S2A). One of these clones (IE7) was injected into C57BL/6J blastocysts and yielded chimeric male offspring that were able to pass the CD137 disruption through the germline after mating with C57BL/6J females. The resulting germline mice were of mixed (C57BL/6J × 129/Sv) background and were expanded as a mixed population for several generations prior to being subjected to speed-backcrossing (using microsatellite markers for BALB/c mice at Charles River Laboratories) for 5 generations to yield mice that were more than 99% BALB/c character. An additional 2 backcrosses were made to inbred BALB/c mice prior to expansion for use in these experiments. Because the entire coding region for CD137 is missing from these mice, there is no CD137 mRNA nor protein present in them (Supplementary Fig. S2B).

All animal procedures were conducted under institutional guidelines that comply with national laws and policies.

The murine endothelial cell line PY-4-1 was kindly provided by V. Bautch (University of North Carolina; ref. 35). The mouse coronary endothelial cells were purified and immortalized by A. Luque (36). In brief, endothelial cells were isolated by positive selection using platelet/endothelial cell adhesion molecule-1 or ICAM-2 (37) antibodies bound to magnetic beads (Dynabeads, Invitrogen). Subconfluent primary cultures were incubated in the presence of polybrene (8 μg/mL; Sigma) with supernatant from packaging cells producing recombinant retroviruses that transduced polyoma middle T antigen (virus concentration, approximately 10–200 pfu/cell).

CT26, EMT6, and Lewis lung carcinoma (LLC) tumor cell lines (38) were from ATCC, and authenticated and quality controlled by the services of the cell bank at Bristol-Myers Squibb by DNA testing. Cells were cultured in complete RPMI medium [RPMI 1640 with Glutamax (Gibco, Invitrogen) containing 10% heat-inactivated FBS (Sigma-Aldrich), 100 IU/mL penicillin and 100 μg/mL streptomycin (Biowhittaker), and 5 × 10^{-5} mol/L 2-mercaptoethanol (Gibco)]. For hypoxic culture conditions, serum-starved PY-4-1 cells, McoECs, and lung primary endothelial cells were incubated for the indicated times under 1% O_2 atmosphere in a modular incubator chamber (Billups-Rothenberg Inc.).

Primary endothelial cells were isolated from lungs of C57BL/6 mice by collagenase digestion followed by selection using Dynabeads Sheep anti-rat IgG (Invitrogen) coupled to a rat anti-mouse ICAM-2 (BD Pharmingen).

In vivo tumor growth and microPET analysis

A total of 0.5 × 10^6 CT26, EMT-6, and LLC cells were injected in 100 mL PBS subcutaneously in the flank. Mice were sacrificed when tumor sizes reached 150 mm^2. Positron emission tomography (PET) analyses showing tumor hypoxia in CT26 established tumors with the radiotracer fluorine-18-fluoromisonidazole (^{18}FMISO) synthesized as described (39).

Mice were injected with ^{18}F-FMISO (14.9 ± 4.9 MBq in 100 μL) in the tail vein. Four hours later, a static 30-minute study (sinogram) was acquired using a Mosaic (Philips) small animal dedicated imaging tomography with 11.9-cm axial field of view (FOV), 12.8-cm transaxial FOV and a 2-mm resolution.

For the assessment of tumor ^{18}F-FMISO uptake, all studies were exported and analyzed using the PMOD software (PMOD Technologies Ltd.). Regions of interest were drawn on coronal 1-mm-thick small-animal PET images on consecutive slices including the entire tumor. Finally, maximum standardized uptake value (SUV) was calculated for each tumor using the formula: SUV = [tissue activity concentration (Bq/cm^3)/injected dose (Bq)] × body weight (g).

Flow cytometry, antibodies, and tissue immunofluorescence

For flow cytometry analysis of tumor endothelial cells, we placed cleanly excised tumor nodules in Petri dishes and minced them finely with a scalpel blade, and incubated them for 45 minutes at 37ºC in a solution containing Collagenase-D and DNAse-I (Roche) in RPMI. We then took the entire material and passed it through a 70-μm cell strainer (BD Falcon, BD Bioscience) pressing with a plunger, to obtain unicellular cell suspensions. Single cell suspensions were pretreated with FcR-Block (anti-CD16/32 clon 2.4G2; BD

Published OnlineFirst February 1, 2011; DOI: 10.1158/0008-5472.CAN-10-1733

Pharmingen). Afterwards, cells were stained with the following antibodies or reagents obtained from BD Pharmingen: CD34-FITC, CD31-PE, CD45.2-APC, CD137-biotin, Syrian Hamster Isotype control-biotin, ICAM-1-biotin, VCAM-1-biotin, E-selectin-biotin, Rat IgG2a, and RatIgG2b biotin conjugated isotype controls. Biotin-conjugated primary antibodies were detected with Streptavidine-APC-Cy7 and 4′,6 diamidino 2 phenylindole was used for dead cell exclusion. Other antibodies used were CD3-FITC, CD8-APC, CD137-PE, and Syrian Hamster Isotype control-PE (BD Pharmingen).

FACS-Canto II and FACSCalibur (BD-Biosciences) were used for cell acquisition and data analysis was carried out using FlowJo software (Tree Star Inc.). For sorting, a FACS-ARIA (BD-Biosciences) was used.

The agonist mouse CD137 clone 1D8 was produced in Chinese hamster ovary (CHO) cells. The heavy and light chain genes for mAb 1D8 were cotransfected into DG44CHO cells maintained in protein-free CHO media (Sigma-Aldrich). Purified anti-CD137 mAb was certified to have less than 0.5 EU/mg endotoxin level, more than 95% purity, and less than 5% high molecular weight species (Bristol-Myers Squibb). Stock solutions of anti-CD137 mAb were kept at −80°C and were thawed on ice prior to use. Polyclonal rat immunoglobulin G (IgG) lipopolysaccharide (LPS)-free was purchased from Sigma (<0.5 EU/mg endotoxin confirmed in our hands).

M-450 tosylactivated Dynabeads (Dynal) coupled with 1D8 anti-CD137 mAb or Rat IgG were used for *in vitro* stimulation of endothelial cells. Antibody coupling to the microbeads was done following the manufacturer's instructions.

Tissue immunofluorescence staining was performed on 10-μm thick cryosections with the following antibodies: anti–ICAM-1-AF647 and anti–VCAM-1-AF647 (Biolegend), CD31-PE (BD Pharmingen), and goat anti-CD137 (R&D Systems) followed by anti-goat AF488 (Invitrogen) antibody in the second step to visualize the antigen. For confocal microscopy, LSM 510 META (Carl Zeiss) equipment was used. The images were analyzed using Zeiss LSM Image Browser software.

Directed *in vivo* angiogenesis assay

Angiogenic responses were compared and quantitated as described previously (40).

In brief, this assay consists of subcutaneous implantation of semiclosed silicone cylinders (angioreactors) filled with CT26 tumor cells embedded in Matrigel (BD Biosciences; Supplementary Fig. S3A). Vascularization within angioreactors was quantified 11 days later by the intravenous injection of the intravascular contrast fluorescein isothiocyanate (FITC)-dextran, followed by spectrofluorimetry on the Matrigel from excised angioreactors (Supplementary Fig. S3B and C). As a positive control of angiogenesis inhibition, the compound 77427 was used (40).

Molecular analyses

Total RNA was extracted from tumor endothelial cells sorted by FACS-Aria (BD Biosciences) using RNAsy Mini Kit (Qiagen). We treated RNA with DNaseI (Gibco-BRL) prior to reverse transcription with Moloney murine leukemia virus (MMLV) reverse transcriptase (Gibco-BRL) in the presence of RNaseOUT (Gibco-BRL). Real-time PCR was done with iQ SYBR green supermix in an iQ5 real-time PCR detection system (Bio-Rad). Copy numbers of CD137 DNA were quantified by quantitative RT-PCR with primers annealing the mouse CD137 cDNA (forward primer: 5′-AACATCTGCAGAGTGTGTGC-3′, reverse primer: 5′-AGACCTTCCGTCTAGAGAGC-3′, product length: 252 bp). PCR amplification was done under the following conditions: 1 cycle of 3 minutes at 95°C; followed by 45 cycles of 30 seconds at 95°C, 15 seconds at 60°C, 30 seconds at 72°C, 25 seconds at 77°C, 10 seconds at 84°C, and 30 seconds at 85°C (detection temperature of 84°C); followed by a single final extension cycle of 72°C for 3 minutes. Immediately after the PCR, a melting curve was generated by raising the incubation temperature from 55°C to 95°C to confirm amplification specificity. The final PCR product was also analyzed by agarose gel electrophoresis. Samples were analyzed in duplicate and data were normalized by comparison with β-actin as an internal control (forward primer: 5′-CGCGTCCACCCGCGAG-3′, reverse primer: 5′-CCTGGTGCCTAGGGCG-3′, product length: 194 bp). The amount of each transcript was expressed according to the formula $2^{Ct\ (\beta\text{-actin})\ -\ Ct(CD137)}$, in which Ct is the point at which the fluorescence increases appreciably above background fluorescence. Primers for amplification of the 2 mCD137 isoforms are 5′-TGTGTGCAGGCTATTTCAGG-3′ and 5′-GAGCTGCTCCAGTGGTCTTC-3′ (35 cycles of 30 seconds at 95°C, 30 seconds at 60°C, 30 seconds at 72°C) with a 2720 Thermal Cycler (Applied Biosystems) and BioTaq DNA Polymerase (Bioline). Isoform 1 product length: 504 bp; isoform 2 product length: 369 bp. PCR products were visualized with SYBR Safe (Invitrogen) after electrophoresis on 1% agarose gels.

Adoptive T-cell transfers

Total splenocytes from *CD137*$^{-/-}$ donor mice were activated with Con-A (10 μg/mL; Sigma), labeled with carboxyfluorescein succinimidyl ester (CFSE) 2.5 μmol/L and inoculated intravenously (10^7 T cells per mouse) into *Rag*$^{-/-}$ recipient mice carrying CT26 flank tumors that had an approximate volume of 100 mm^2.

We treated recipient mice with anti-CD137 1D8 (100 μg per mouse) or LPS-free NA/LE Rat IgG as control for 48 hours before T-cell transfer. In some experiments, we treated mice i.p. with a neutralizing antibody against mouse ICAM-1 (50 μg per mouse, clone YN1/1.7.4; Biolegend) and against mouse VCAM-1 (50 μg per mouse, clone M/K-1.9). We harvested tumors 48 hours after T-cell transfer, and analyzed them for CFSE and CD8-APC in a FACS Canto II flow cytometer. Absolute numbers of infiltrating T cells were calculated and referred to the total number of lymphocytes counted per cell suspension (Z1 Coulter Particle Counter, Beckman Coulter).

Statistical analysis

Prism software (Graph Pad Software) was used to analyze the quantitative PCRs, directed *in vivo* angiogenesis assay, adhesion molecule induction and tumor infiltration data, and to determine statistical significance of the differences between groups by applying unpaired Student's *t* tests or 2- way ANOVA tests. $P < 0.05$ was considered significant.

Published OnlineFirst February 1, 2011; DOI: 10.1158/0008-5472.CAN-10-1733

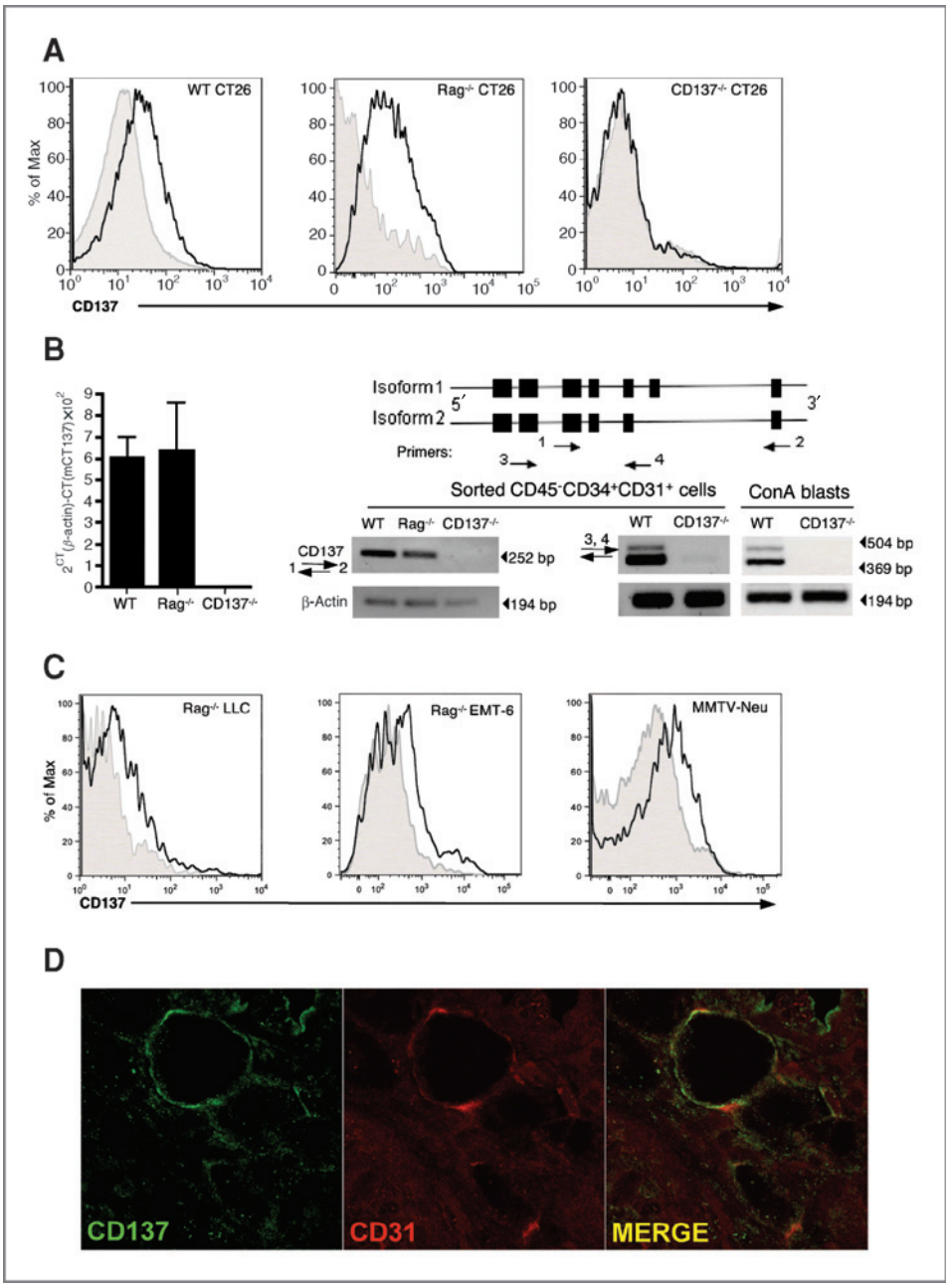

Figure 1. Expression of CD137 on mouse tumoral endothelial cells. A, multicolor FACS expression analysis of surface CD137 on $CD45^{-}CD31^{+}CD34^{+}$-gated cells in unicellular suspensions obtained from CT26 colon carcinomas s.c. grafted in BALB/c (WT, Rag $^{-/-}$, or $CD137^{-/-}$) mice as indicated in the figure. Shaded histograms represent isotype matched control mAb. Results are representative of 4 independent experiments. B, left, quantitative RT-PCRs with CD137 specific primers on RNA obtained from FACS sorted $CD45^{-}CD34^{+}CD31^{+}$ cells to more than 98% purity from cell suspensions as in A. Results are representative of 3 experiments similarly done. Right, the RT-PCR products were amplified with the indicated pairs of CD137-specific primers and β-actin as a control. Primers 1, 2 and 3, 4 amplify transcripts corresponding to the isoforms 1 and 2, respectively. RNA was obtained from FACS-sorted tumor endothelial cells or BALB/c splenocytes activated for 72 hours with concanavalin-A (con-A blasts). C, CD137 surface expression on $CD45^{-}CD34^{+}CD31^{+}$ endothelial cells in LLC, and EMT-6 derived tumors grafted s.c. in Rag $^{-/-}$ mice. The right FACS histogram shows CD137 expression in unicellular suspensions obtained from spontaneous tumor nodules derived from MMTV-HER2 transgenic mice. Results shown are representative of at least 3 that rendered similar results. D, tissue immunofluorescence confocal microphotographs showing staining for CD31 (red) and CD137 (green). The right picture is an overlay (merge) that shows colocalization.

Results

CD137 protein is expressed on endothelial cells in mouse tumors

To ascertain whether CD137 protein was present on tumor endothelial cells, a multicolor staining strategy was performed on unicellular suspensions obtained from syngeneic tumors grafted in mice. Supplementary Figure S1 shows the strategy to gate $CD45^{-}CD31^{+}CD34^{+}$. When those cells from CT26 colon carcinomas were costained with anti-CD137 mAb, surface expression was indeed observed. Such costaining was preserved when tumor cells were grafted in T- and B-cell–deficient immunodeficient *Rag*$^{-/-}$ mice (Fig. 1A). To ensure immunostaining specificity, mice whose CD137 gene had been silenced were used (Supplementary Fig. S2). In this case, $CD45^{-}CD34^{+}CD31^{+}$ endothelial cells did not show reactivity to anti-CD137 mAb on multicolor FACS staining.

Moreover, when such $CD45^{-}CD34^{+}CD31^{+}$ endothelial cells were sorted by FACS, mRNA encoding for CD137 was detected by quantitative RT-PCR (Fig. 1B). Interestingly, the 2 differentially spliced transcripts were detected in tumor endothelial cells (Fig. 1B) using primers that amplify both cDNAs as they do in spleen T cells activated with concanavalin-A (Fig. 1B). This is of interest because the shorter transcript has been found to encode for a soluble form of CD137, whose function is unclear even in the case of T lymphocytes (41). RT-PCR bands

Published OnlineFirst February 1, 2011; DOI: 10.1158/0008-5472.CAN-10-1733

were thoroughly sequenced to confirm CD137 identity (data not shown).

To rule out the possibility that this was a feature exclusive to CT26-derived tumors implanted in BALB/c mice, we conducted similar experiments with grafts of LLC and EMT6 breast carcinoma implanted in C57BL6 and BALB/c mice respectively. In these tumors, specific immunostaining was also documented with anti-CD137 mAb. (Fig. 1C). Moreover, expression of CD137 was found on the $CD45^{-}CD31^{+}CD34^{+}$ cells from spontaneous breast carcinomas (Fig. 1C) arising in MMTV-HER-2 transgenic mice (34). Therefore, the expression of CD137 on endothelium is not an exclusive characteristic of transplanted tumors.

In surgically excised CT26 tumors, it was possible to document by tissue immunofluorescence under confocal microscopy that most $CD31^{+}$ cells in vascular structures are costained with anti-CD137 further confirming the presence of CD137 in tumor-associated vascular endothelium (Fig. 1D).

Hypoxia induces CD137 on mouse endothelial cells

The expression of CD137 on mouse endothelial cells from tumors raised the question of which microenvironmental factor would drive CD137 expression. Tumors constitute a hypoxic tissue as we observe in CT26 established tumors using a PET technique that visualizes hypoxia as a result of FMISO retention (Fig. 2A). We found that the endothelioma cell line PY-4-1(35) does not express surface CD137. However, if these cells are cultured for 24 hours in a 1% O_2 hypoxia chamber, immunostaining with anti-CD137 mAbs becomes apparent (Fig. 2B). PY-4-1 is derived from hemangiomas arising in SV40 T transgenic mice. To check whether this could be seen in other mouse endothelial cells, a cell line immortalized in culture from coronary endothelium by SV40 T Ag transfection (42) was used rendering similar results (Fig. 2C). Induction of CD137 expression took place at the transcriptional level as it could be observed in quantitative RT-PCRs (Fig. 2D).

However, it could be argued that CD137 upregulation in response to hypoxia might be caused by the transformed nature of the endothelial cell lines used in Figure 2. To exclude this interpretation, experiments were done on short-passaged primary endothelial cells isolated from mouse lungs that showed upregulation of surface CD137 (Fig. 3A) and CD137 mRNA (Fig. 3B) in response to hypoxia.

Lack of antiangiogenic effects of anti-CD137 mAb

Our findings on selectively CD137 expression on tumor endothelium suggested that perhaps part of the therapeutic effects of anti-CD137 mAb could be attributed to antiangiogenesis or other effects on tumor vascularization.

However, when mice were implanted with mm-sized tubes filled with CT26 cells embedded in Matrigel, anti-CD137 treatment showed a degree of vascularization similar to that found with control antibody. These experiments shown in Supplementary Figure S3 were done in $Rag^{-/-}$ mice to rule out any indirect effects mediated by $CD8^{+}$ T cells. The method for vascularization analysis was based on measuring an intravascular fluorescent dye inside the excised Matrigel tubes. The amount of vascularization of the Matrigel implants was

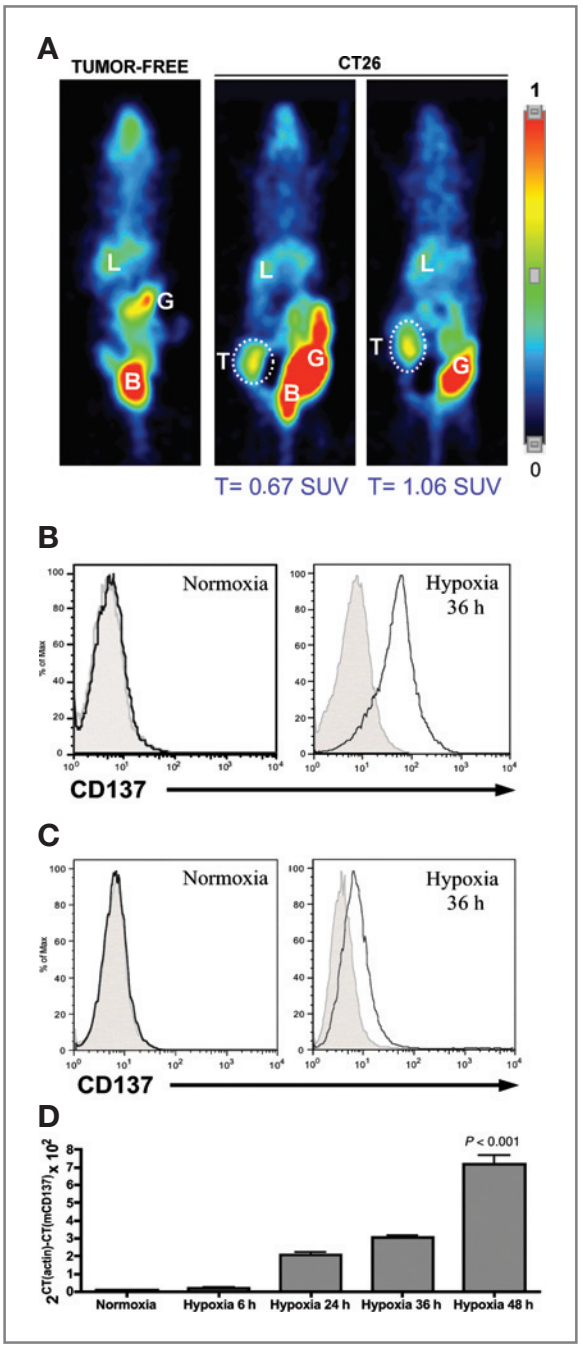

Figure 2. Hypoxia induces CD137 expression in mouse endothelial cells. A, ^{18}FMISO microPET imaging of mice harboring established CT26 tumors in the right flank. Tumors are gated and SUV in the gated regions are provided under the corresponding pictures. T indicates tumor, B bladder, L liver, and G gut. B, PY-4-1 endothelioma cells were cultured for 24 hours in normoxia and 1% O_2 atmosphere. CD137 surface expression was studied using direct immunofluorescence in normoxic or hypoxic cells as indicated in the figure. Shaded histograms represent staining with isotype-matched control antibody. Experiments are representative of 3 similarly conducted. C, MCoEC cells derived from coronary endothelium immortalized by stable transfection of SV40T were cultured and studied for CD137 as in A. This experiment was repeated twice rendering similar results. D, quantitative RT-PCR studied on RNA extracted from PY-4-1 cells cultured under 1% O_2 hypoxia for the indicated periods of time.

Published OnlineFirst February 1, 2011; DOI: 10.1158/0008-5472.CAN-10-1733

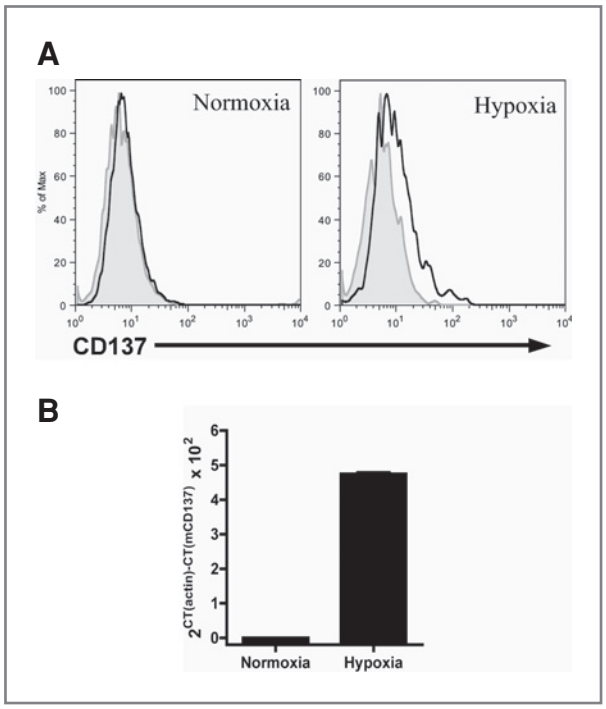

Figure 3. Hypoxia upregulates CD137 in mouse primary endothelial cells from the lung. Primary endothelial cells were isolated from disaggregated mouse lung tissue and cultured for 3 passages before being subjected or not to 1% hypoxia for 48 hours. Surface expression of CD137 (A) and mRNA encoding CD137 (B) were measured as in Figure 2.

similar in CD137$^{-/-}$ mice indicating a nondefective vascularization, that indeed could be suppressed by the well-described antiangiogenic drug 77427 (40) used as a positive control.

CD137 ligation on endothelial cells increases expression of lymphocyte-homing adhesion molecules

An attractive hypothesis was that if CD137 on endothelial cells were coupled to the same signal transduction machinery as in T-cells, this could drive proinflammatory changes. Indeed, when PY-4-1 endothelioma cells were cultured under hypoxia and treated with 4.5-μm diameter microbeads coated with the agonist anti-CD137 mAb 1D8, expression of E-selectin, VCAM-1, and ICAM-1 were upregulated (Fig. 4A; Supplementary Fig. S4). Agonist anti-CD137 antibody-coated microbeads were chosen to mimic cells expressing CD137L.

If these mechanisms occurred *in vivo*, the expression of adhesion molecules could facilitate infiltration of T lymphocytes into tissues. To verify whether this mechanism was actually at work *in vivo*, experiments in BALB/c mice grafted with CT26 tumors were done. Accordingly, mice with 10-mm mean diameter tumors were treated with 1D8 anti-CD137 mAb or control rat IgG. Both antibodies were devoid of LPS. As can be seen in Figure 4B, the immunostaining in CD45$^-$CD34$^+$CD31$^+$ cells for ICAM-1, VCAM-1, and E-selectin dramatically increased. To exclude events related to T cells and to ensure that the observations were due to CD137 ligation, experiments were carried out in *Rag*$^{-/-}$ and *CD137*$^{-/-}$ mice. Figure 4C shows that no upregulation took place in *CD137*$^{-/-}$ mice, but upregulation was readily seen in T/B-cell–deficient *Rag*$^{-/-}$ mice.

Confocal microscopy examination of tumor tissue samples from *Rag*$^{-/-}$ mice treated with anti-CD137 mAb showed ICAM-1 and VCAM-specific immunofluorescence associated to capillary walls (Fig. 4D).

Our interpretation is that ligation of CD137 on mouse tumor endothelial cells gives rise to signals that enhance the expression of lymphocyte homing molecules.

Treatment with anti-CD137 mAb increases T-cell homing into tumors as a result of a direct stimulation of endothelial cells

The next question was to ascertain whether CD137 upregulation of homing receptors on endothelial cells actually gave rise to enhanced intratumoral infiltration of activated T lymphocytes.

For this purpose, as depicted in Figure 4A, Con-A T-cell blasts were prepared from the spleen of *CD137*$^{-/-}$ syngenic mice (Supplementary Fig. S2) and labeled with CFSE. *Rag*$^{-/-}$ mice harboring CT26 tumors were used as recipients for the *CD137*$^{-/-}$ Con-A T-cell blasts. Mice had been pretreated with anti-CD137 mAb or control antibody as presented in the scheme (Fig. 5A).

As seen in Figure 5B, many more fluorescent cells were recovered from unicellular suspensions of the CT26 tumors 2 days later on treatment with anti-CD137 mAb. Given that the antitumor immunotherapeutic effects of anti-CD137 mAb are mostly attributed to CD8 T cells, it was also important to verify that CD8$^+$ CFSE$^+$ T cells entered more avidly into the tumor tissue as shown in Figure 5C. Similar data have been observed in LLC tumors transfected to express ovalbumin when transferring anti-OVA TCR transgenic CD8$^+$ T cells (Supplementary Fig. S5) indicating that tumor antigen-specific T cells can also enter more efficiently to tumors under treatment with anti-CD137 mAb. Other groups have also reported enhanced entrance of tumor antigen-specific T cells on anti-CD137 mAb treatment (43)

In the experiments shown in Figure 5B and C, we observed that pretreatment of the mice with a mixture of anti–ICAM-1 and anti–VCAM-1 blocking mAbs almost completely blocked the entrance of *CD137*$^{-/-}$ fluorescent T-cell blasts.

Discussion

Traffic of T cells into tumors is a limiting factor for the efficacy of immunotherapy that can spoil the results of cancer vaccines and adoptive T-cell therapies even in the cases when tangible cellular immune responses are present in peripheral blood (44). Local proinflammatory cytokines (45) including TNFα, IFNγ, interleukin (IL)-1, and CD40 ligation (46) enhance the expression of homing receptors for activated T lymphocytes on endothelial cells. In this study, we found that CD137 protein and mRNA are functionally expressed by endothelial cells harvested from mouse solid tumors. Importantly, CD137 ligation on tumor endothelial cells triggers proinflammatory changes in the tumor vasculature that recruit T cells toward malignant tissue.

Published OnlineFirst February 1, 2011; DOI: 10.1158/0008-5472.CAN-10-1733

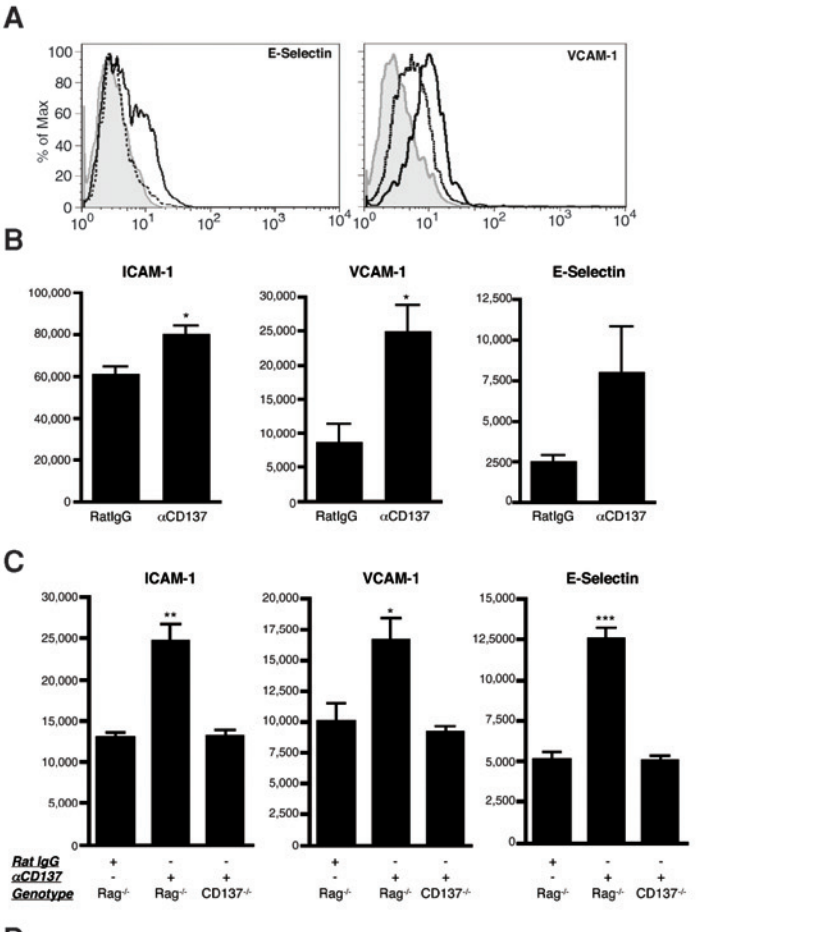

Figure 4. CD137 ligation on tumor endothelial cells increases expression of lymphocyte homing receptors. A, PY-4-1 cells cultured on hypoxia for 36 hours and exposed to 4.5-μm diameter latex beads coated with anti-CD137 1D8 mAb (continuous line histograms) or control antibody (dotted histograms) at a 1:10 bead/cell ratio. After culture, cells were studied by FACS for expression E-selectin and VCAM-1 as indicated in the figure. Shaded histograms represent negative control immunostaining with isotype matched irrelevant mAbs. Data are representative of 3 experiments. Mean ± SD of these independent experiments is presented as Supplementary Figure S4. B, BALB/c mice bearing CT26 tumors (8–12 mm in diameter) were treated with RatIgG or αCD137 1D8 mAb. Tumors were excised 36 hours later and cell suspensions were analyzed for the indicated markers on $CD45^{-}CD34^{+}CD31^{+}$-gated endothelial cells. Results represent the mean intensity of immunofluorescence ± SD in 3 experiments with 3 mice per group. C, experiments as in B but done in the indicated strains of mice ($Rag^{-/-}$ and $CD137^{-/-}$ as indicated). Data represent the mean intensity of immunofluorescence ± SD in 3 experiments with 3 mice per group. D, tissue immunofluorescence experiments visualized by confocal microscopy showing colocalization of CD31 with ICAM-1 or VCAM-1 in CT-26 tumors implanted in syngeneic $Rag^{-/-}$ mice and treated 1 day before with 100 μg of anti-CD137 mAb.

Published OnlineFirst February 1, 2011; DOI: 10.1158/0008-5472.CAN-10-1733

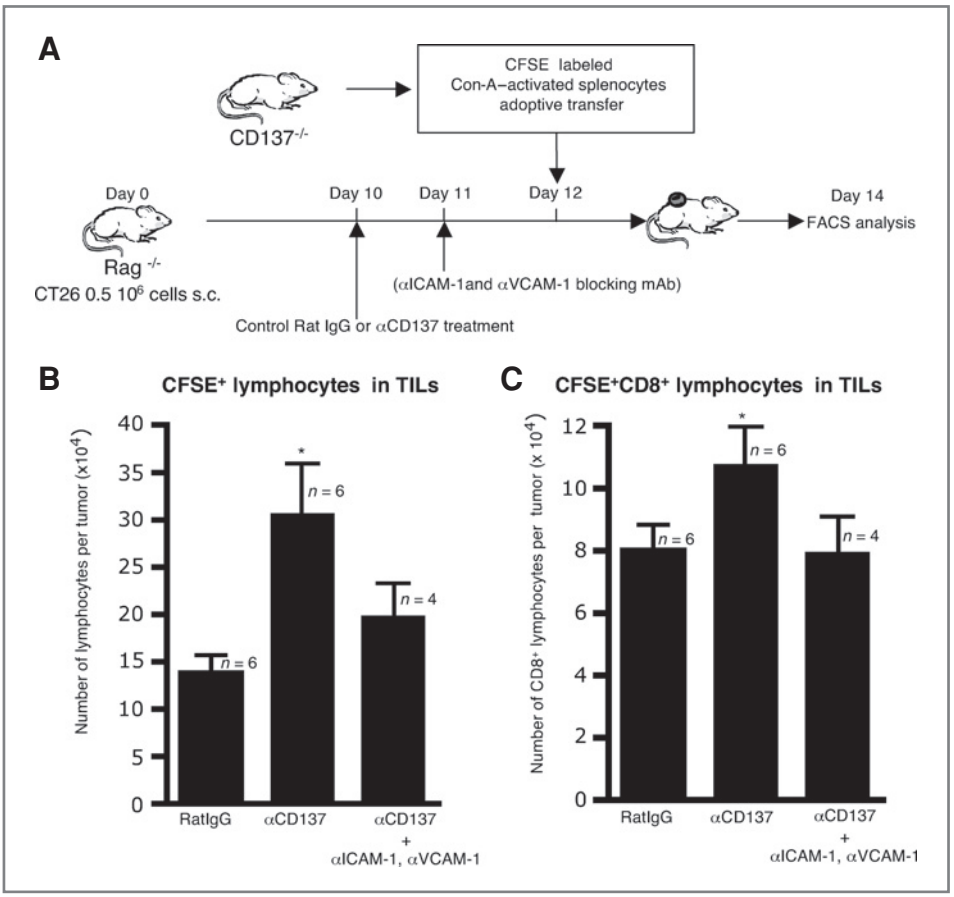

Figure 5. Treatment with anti-CD137 agonist mAb induces T-cell homing into tumor lesions. A, schematic representation of the experimental procedures. Rag$^{-/-}$ mice were grafted with CT26 tumors and treated with 100 μg of RatIgG or αCD137 mAb 1D8. One day later, some of the mice were i.p. injected with a mixture of anti–ICAM-1 and anti–VCAM-1 neutralizing mAb. Twenty-four hours later, all mice received 10^7 T-cell blasts activated with 10 μg/mL of Con-A. Con-A blasts were derived from the spleen of syngenic CD137$^{-/-}$ mice and were labeled with CFSE prior to i.v. adoptive transfer. FACS analysis of tumor infiltrating lymphocytes (TIL) was done 2 days after adoptive transfer. B, quantitation of CFSE$^+$ events in cell suspensions obtained from tumors treated as indicated in A. Data represent mean ± SD from an experiment out of 3 rendering comparable results. C, CD8$^+$-gated CFSE$^+$ events analyzed by FACS multicolor analysis from the same samples as in B.

Previous reports had advanced evidence for the expression of CD137 on vascular cells. This includes human tumor vessels (10) and inflamed atherosclerotic lesions (11, 47). Immunohistochemical evidence for CD137 expression in capillaries from a number of human malignant tumors had been reported, although benign neoplasms tended to show no anti-CD137 immunostaining in vessels (10). In mice, CD137-encoding mRNA has been found in mouse tumor endothelial cells purified by multistep immunomagnetic procedures from tumor vessels, but not from angiogenic vascular cells obtained from regenerating liver (9). In this study, we provide evidence for functional protein expression at the tumor endothelial cell surface. Expression of CD137 on mouse tumor vessels seems to be a common feature that includes a variety of transplantable tumors and spontaneous carcinomas arising in oncogene transgenic mice.

The tumor microenviroment is known to be hypoxic, as we confirm by PET imaging (39). Hypoxia controls many phenotypic features of endothelial cells. Thus, it could be hypothesized that CD137 expression on endothelial cells could be driven by hypoxia. We have observed that mouse endothelial cells subjected to hypoxia expressed surface CD137, whereas it was absent in normoxic conditions of culture. When analyzing the locus of mouse CD137 (GenBank accession number NC_000070), we have identified several putative hypoxia response elements. The focus of our currently ongoing research (A. Palazon and colleagues, manuscript in preparation) is to specifically explore the role of hypoxia in controlling CD137 expression in immune and nonimmune cells. The fact that CD137 is not expressed in a normoxic atmosphere indicates that CD137 would be selectively upregulated in tissues suffering lack of oxygen supply such as the tumor microenvironment, healing wounds, ischemia-atherosclerosis conditions. Therefore, the importance of these findings goes beyond tumor immunotherapy. The nature of the CD137L$^+$ cells that would naturally stimulate CD137 on the hypoxic endothelial cells remains elusive, but in atherosclerotic lesions has been proposed to be a subset of activated macrophages (47).

Two important conclusions can be drawn from selective expression in tumor vessels: (i) the tumor endothelium would offer CD137 as a selective marker for targeted therapies, and (ii) selective tissue distribution would confine the vascular effects of CD137-stimulation inside the malignancy, thereby avoiding systemic side effects.

Our series of angiogenesis assessments concluded that there were no detectable antiangiogenic effects *in vivo* by the anti-CD137 mAb. This was consistent with previous results measuring angiogenesis in nude mice implanted with Matrigel plugs containing VEGF and b-FGF (data not shown). In

Published OnlineFirst February 1, 2011; DOI: 10.1158/0008-5472.CAN-10-1733

addition, anti-CD137 mAb have never induced any tumor shrinkage when tumors are implanted in T-cell–deficient mice. For this reason, our angiogenesis experiments have been carried out in *Rag*$^{-/-}$ to avoid any antivascularization effects indirectly mediated by lymphocytes whose function was going to be otherwise enhanced via CD137. According to these negative results, the primary therapeutic effects of anti-CD137 mAb cannot be attributed to downregulation of angiogenesis or vasculogenesis.

What we have observed is that CD137 cross-linking at the surface of endothelial cells gives rise to upregulated expression of VCAM-1, ICAM-1, and E-selectin. These observations are consistent with previous findings in atherosclerotic lesions in mice on treatment with anti-CD137 mAb (11). These homing molecules acting in a concerted fashion with chemokines are key mediators in the recruitment of an inflammatory infiltrate (33). Primed lymphocytes bear activated LFA-1 and VLA-4 integrins that would avidly interact with their counter-receptors, thereby to mediate extravasation. Contrary to what happens with CD40 or proinflammatory cytokine receptors, CD137 is selectively expressed on tumor vasculature and thus the observed proinflammatory changes ought to take place selectively at the tumor lesion. However, these proadhesive effects of agonist anti-CD137 mAb can also occur in atherosclerotic lesions (11) and therefore attention must be paid to cardiovascular events in clinical trials, particularly when considering patients with vascular risk factors.

The ICAM-1 and VCAM-mediated enhanced entrance of lymphocytes into tumors could define an additional antitumor mechanism of action of the immunostimulatory anti-CD137 mAb. Such a mechanism would not be alternative, but complementary to the costimulatory effects of the anti-CD137 agonist antibodies on T cells. The vascular effects could be considered an independent mechanism of action, as we observed migration of *CD137*$^{-/-}$ activated lymphocytes that are unresponsive to the agonist anti-CD137 mAb.

We had found a similar antitumoral mechanism of action depending on VCAM upregulation by confining IL-12 expression to tumor nodules by means of gene therapy (48, 49). Because agonist antibodies directed to OX40, CD27, and GITR exert immunotherapeutic effects (17), it would be of much interest to ascertain whether any of these members of the TNF-receptor family with homology with CD137 are also functionally expressed, at least in some cases, on tumor endothelial cells. If this is the case, agonist mAb against such molecules could share to some extent this mechanism of action.

In the case of CD137-targeted therapies, a multilayered mechanism of action emerges in which actions on immune cells and endothelium could synergistically contribute to the therapeutic effects. We postulate that vascular and immune mechanisms may act in a mutually cooperative manner, as the most intensely activated lymphocytes will be selectively recruited by adhesion molecules elicited at the lumen of blood vessels irrigating tumor lesions. In turn, the growing T-cell infiltrate costimulated via CD137 would further enhance local inflammation by more intensely producing chemokines and proinflammatory cytokines. In this regard, the effects on tumor endothelium contribute to explain the observed synergies of anti-CD137 mAb treatment with cancer vaccines (17, 18) and adoptive transfers of activated T cells (19, 50).

Our data are very much in agreement with recent elegant experiments by the group of L. Chen (50) with mouse bone marrow chimeras that advocate an involvement of a CD137-expressing nonhematopoietic cell component in the therapeutic mechanism of action of anti-CD137 mAb against B16-OVA derived melanomas. Moreover, we have observed that in a synergistic combination of adoptive transfer of activated tumor specific CD8 T cells plus anti-CD137 mAb treatment, the synergistic curative effects are not observed if the host animal is *CD137*$^{-/-}$ indicating that other recipient cells expression CD137 beyond the transferred T cells are absolutely required (Marinez-Forero and colleagues, manuscript in preparation). Further research will establish which lymphocyte subsets are recruited to the tumor microenvironment on CD137 stimulation of tumor endothelium. It might be that not only effector lymphocytes, but also regulatory T cells could be invited to enter the tumor. If this is the case, elimination of Treg cells concomitantly to CD137 therapeutic stimulation may be advisable as recently observed by the group of Ronald Levy (51).

Taking collectively, these data point to a model in which the tumor vascular response to anti-CD137 agonist mAb can be considered an additional and important element in the multilayered mechanisms of action against tumors elicited by these promising immunotherapeutic agents (3).

Disclosure of Potential Conflicts of Interest

M. Jure-Kunkel and J. Dinchuk are full-time employees of Bristol-Myers Squibb. I. Melero has received consultancy honoraria and reagents from Bristol-Myers Squibb.

Acknowledgments

We thank Dr. Lieping Chen (Johns Hopkins, Baltimore) for long-term collaborations on CD137 and Dr. Jesus Prieto (Universidad de Navarra) for scientific discussion. We also thank Izaskun Gabari for technical support with FACS experiment, and Eneko Elizalde and Elena Ciordia for excellent animal care.

Grant Support

Financial support was from MEC/MICINN (SAF2005-03131 and SAF2008-03294), Departamento de Educación del Gobierno de Navarra, Departamento de Salud del Gobierno de Navarra (Beca Ortiz de Landázuri), Caja de ahorros de Navarra (CAN), Redes temáticas de investigación cooperativa RETIC (RD06/0020/0065), European commission VII framework program (ENCITE), SUDOE-IMMUNONET, and "UTE for project FIMA". S.H-S. has a Ramon y Cajal contract from MICINN and A. Palazón a scholarship from FIS. A. Morales-Kastresana receives a FPI scholarship from MICINN.

The costs of publication of this article were defrayed in part by the payment of page charges. This article must therefore be hereby marked *advertisement* in accordance with 18 U.S.C. Section 1734 solely to indicate this fact.

Received May 14, 2010; revised November 29, 2010; accepted November 30, 2010; published OnlineFirst January 25, 2011.

Published OnlineFirst February 1, 2011; DOI: 10.1158/0008-5472.CAN-10-1733

References

1. Watts TH. TNF/TNFR family members in costimulation of T cell responses. Annu Rev Immunol 2005;23:23–68.
2. Croft M. The role of TNF superfamily members in T-cell function and diseases. Nat Rev Immunol 2009;9:271–85.
3. Melero I, Murillo O, Dubrot J, Hervas-Stubbs S, Perez-Gracia JL. Multi-layered action mechanisms of CD137 (4-1BB)-targeted immunotherapies. Trends Pharmacol Sci 2008;29:383–90.
4. Melero I, Johnston JV, Shufford WW, Mittler RS, Chen L. NK1.1 cells express 4-1BB (CD137) costimulatory molecule and are required for tumor immunity elicited by anti-4-1BB monoclonal antibodies. Cell Immunol 1998;190:167–72.
5. Choi BK, Kim YH, Kwon PM, Lee SC, Kang SW, Kim MS, et al. 4-1BB functions as a survival factor in dendritic cells. J Immunol 2009; 182:4107–15.
6. Nishimoto H, Lee SW, Hong H, Potter KG, Maeda-Yamamoto M, Kinoshita T, et al. Costimulation of mast cells by 4-1BB, a member of the tumor necrosis factor receptor superfamily, with the high-affinity IgE receptor. Blood 2005;106:4241–8.
7. Zhang X, Voskens CJ, Sallin M, Maniar A, Montes CL, Zhang Y, et al. CD137 promotes proliferation and survival of human B cells. J Immunol 2010;184:787–95.
8. Lee SW, Park Y, So T, Kwon BS, Cheroutre H, Mittler RS, et al. Identification of regulatory functions for 4-1BB and 4-1BBL in myelopoiesis and the development of dendritic cells. Nat Immunol 2008;9:917–26.
9. Seaman S, Stevens J, Yang MY, Logsdon D, Graff-Cherry C, St Croix B. Genes that distinguish physiological and pathological angiogenesis. Cancer Cell 2007;11:539–54.
10. Broll K, Richter G, Pauly S, Hofstaedter F, Schwarz H. CD137 expression in tumor vessel walls. High correlation with malignant tumors. Am J Clin Pathol 2001;115:543–9.
11. Olofsson PS, Soderstrom LA, Wagsater D, Sheikine Y, Ocaya P, Lang F, et al. CD137 is expressed in human atherosclerosis and promotes development of plaque inflammation in hypercholesterolemic mice. Circulation 2008;117:1292–301.
12. McNamara JO, Kolonias D, Pastor F, Mittler RS, Chen L, Giangrande PH, et al. Multivalent 4-1BB binding aptamers costimulate CD8+ T cells and inhibit tumor growth in mice. J Clin Invest 2008;118:376–86.
13. Mittler RS, Foell J, McCausland M, Strahotin S, Niu L, Bapat A, et al. Anti-CD137 antibodies in the treatment of autoimmune disease and cancer. Immunol Res 2004;29:197–208.
14. Melero I, Shuford WW, Newby SA, Aruffo A, Ledbetter JA, Hellstrom KE, et al. Monoclonal antibodies against the 4-1BB T-cell activation molecule eradicate established tumors. Nat Med 1997;3:682–5.
15. Yang Y, Yang S, Ye Z, Jaffar J, Zhou Y, Cutter E, et al. Tumor cells expressing anti-CD137 scFv induce a tumor-destructive environment. Cancer Res 2007;67:2339–44.
16. Wilcox RA, Tamada K, Flies DB, Zhu G, Chapoval AI, Blazar BR, et al. Ligation of CD137 receptor prevents and reverses established anergy of CD8+ cytolytic T lymphocytes in vivo. Blood 2004;103:177–84.
17. Melero I, Hervas-Stubbs S, Glennie M, Pardoll DM, Chen L. Immunostimulatory monoclonal antibodies for cancer therapy. Nat Rev Cancer 2007;7:95–106.
18. Ito F, Li Q, Shreiner AB, Okuyama R, Jure-Kunkel MN, Teitz-Tennenbaum S, et al. Anti-CD137 monoclonal antibody administration augments the antitumor efficacy of dendritic cell-based vaccines. Cancer Res 2004;64:8411–9.
19. May KF Jr, Chen L, Zheng P, Liu Y. Anti-4-1BB monoclonal antibody enhances rejection of large tumor burden by promoting survival but not clonal expansion of tumor-specific CD8+ T cells. Cancer Res 2002;62:3459–65.
20. Tirapu I, Arina A, Mazzolini G, Duarte M, Alfaro C, Feijoo E, et al. Improving efficacy of interleukin-12-transfected dendritic cells injected into murine colon cancer with anti-CD137 monoclonal antibodies and alloantigens. Int J Cancer 2004;110:51–60.
21. Kim YH, Choi BK, Kim KH, Kang SW, Kwon BS. Combination therapy with cisplatin and anti-4-1BB: synergistic anticancer effects and amelioration of cisplatin-induced nephrotoxicity. Cancer Res 2008;68:7264–9.
22. Uno T, Takeda K, Kojima Y, Yoshizawa H, Akiba H, Mittler RS, et al. Eradication of established tumors in mice by a combination antibody-based therapy. Nat Med 2006;12:693–8.
23. Seo SK, Choi JH, Kim YH, Kang WJ, Park HY, Suh JH, et al. 4-1BB-mediated immunotherapy of rheumatoid arthritis. Nat Med 2004; 10:1088–94.
24. Myers LM, Vella AT. Interfacing T-cell effector and regulatory function through CD137 (4-1BB) co-stimulation. Trends Immunol 2005;26: 440–6.
25. Sun Y, Chen HM, Subudhi SK, Chen J, Koka R, Chen L, et al. Costimulatory molecule-targeted antibody therapy of a spontaneous autoimmune disease. Nat Med 2002;8:1405–13.
26. Zhang B, Maris CH, Foell J, Whitmire J, Niu L, Song J, et al. Immune suppression or enhancement by CD137 T cell costimulation during acute viral infection is time dependent. J Clin Invest 2007;117:3029–41.
27. Niu L, Strahotin S, Hewes B, Zhang B, Zhang Y, Archer D, et al. Cytokine-mediated disruption of lymphocyte trafficking, hemopoiesis, and induction of lymphopenia, anemia, and thrombocytopenia in anti-CD137-treated mice. J Immunol 2007;178:4194–213.
28. Dubrot J, Milheiro F, Alfaro C, Palazon A, Martinez-Forero I, Perez-Gracia JL, et al. Treatment with anti-CD137 mAbs causes intense accumulations of liver T cells without selective antitumor immunotherapeutic effects in this organ. Cancer Immunol Immunother 2010; 59:1223–33.
29. Lynch DH. The promise of 4-1BB (CD137)-mediated immunomodulation and the immunotherapy of cancer. Immunol Rev 2008; 222:277–86.
30. Martinet O, Ermekova V, Qiao JQ, Sauter B, Mandeli J, Chen L, et al. Immunomodulatory gene therapy with interleukin 12 and 4-1BB ligand: long- term remission of liver metastases in a mouse model. J Natl Cancer Inst 2000;92:931–6.
31. Saoulli K, Lee SY, Cannons JL, Yeh WC, Santana A, Goldstein MD, et al. CD28-independent, TRAF2-dependent costimulation of resting T cells by 4-1BB ligand. J Exp Med 1998;187:1849–62.
32. Jang IK, Lee ZH, Kim YJ, Kim SH, Kwon BS. Human 4-1BB (CD137) signals are mediated by TRAF2 and activate nuclear factor-kappa B. Biochem Biophys Res Commun 1998;242:613–20.
33. Springer TA. Traffic signals for lymphocyte recirculation and leukocyte emigration: the multistep paradigm. Cell 1994;76:301–14.
34. Boggio K, Nicoletti G, Di Carlo E, Cavallo F, Landuzzi L, Melani C, et al. Interleukin 12-mediated prevention of spontaneous mammary adenocarcinomas in two lines of Her-2/neu transgenic mice. J Exp Med 1998;188:589–96.
35. Dubois NA, Kolpack LC, Wang R, Azizkhan RG, Bautch VL. Isolation and characterization of an established endothelial cell line from transgenic mouse hemangiomas. Exp Cell Res 1991;196:302–13.
36. Hortelano S, Lopez-Fontal R, Traves PG, Villa N, Grashoff C, Bosca L, et al. ILK mediates LPS-induced vascular adhesion receptor expression and subsequent leucocyte trans-endothelial migration. Cardiovasc Res 2010;86:283–92.
37. Melero I, Gabari I, Corbi AL, Relloso M, Mazzolini G, Schmitz V, et al. An anti-ICAM-2 (CD102) monoclonal antibody induces immune-mediated regressions of transplanted ICAM-2-negative colon carcinomas. Cancer Res 2002;62:3167–74.
38. Tirapu I, Huarte E, Guiducci C, Arina A, Zaratiegui M, Murillo O, et al. Low surface expression of B7-1 (CD80) is an immunoescape mechanism of colon carcinoma. Cancer Res 2006;66:2442–50.
39. Chang CW, Chou TK, Liu RS, Wang SJ, Lin WJ, Chen CH, et al. A robotic synthesis of [18F]fluoromisonidazole ([18F]FMISO). Appl Radiat Isot 2007;65:682–6.
40. Martinez A, Zudaire E, Julian M, Moody TW, Cuttitta F. Gastrin-releasing peptide (GRP) induces angiogenesis and the specific GRP blocker 77427 inhibits tumor growth in vitro and in vivo. Oncogene 2005;24:4106–13.
41. Shao Z, Sun F, Koh DR, Schwarz H. Characterisation of soluble murine CD137 and its association with systemic lupus. Mol Immunol 2008;45:3990–9.
42. Hortelano S, Lopez-Fontal R, Traves PG, Villa N, Grashoff C, Bosca L, et al. ILK mediates LPS-induced vascular adhesion

Published OnlineFirst February 1, 2011; DOI: 10.1158/0008-5472.CAN-10-1733

receptor expression and subsequent leucocyte trans-endothelial migration. Cardiovasc Res 2010;86:283–92.

43. Wilcox RA, Flies DB, Wang H, Tamada K, Johnson AJ, Pease LR, et al. Impaired infiltration of tumor-specific cytolytic T cells in the absence of interferon-gamma despite their normal maturation in lymphoid organs during CD137 monoclonal antibody therapy. Cancer Res 2002;62:4413–8.
44. Buckanovich RJ, Facciabene A, Kim S, Benencia F, Sasaroli D, Balint K, et al. Endothelin B receptor mediates the endothelial barrier to T cell homing to tumors and disables immune therapy. Nat Med 2008;14:28–36.
45. Pober JS, Sessa WC. Evolving functions of endothelial cells in inflammation. Nat Rev Immunol 2007;7:803–15.
46. Chiodoni C, Iezzi M, Guiducci C, Sangaletti S, Alessandrini I, Ratti C, et al. Triggering CD40 on endothelial cells contributes to tumor growth. J Exp Med 2006;203:2441–50.
47. Jeon HJ, Choi JH, Jung IH, Park JG, Lee MR, Lee MN, et al. CD137 (4-1BB) deficiency reduces atherosclerosis in hyperlipidemic mice. Circulation 2010;121:1124–33.
48. Sangro B, Melero I, Qian C, Prieto J. Gene therapy of cancer based on interleukin 12. Curr Gene Ther 2005;5:573–81.
49. Mazzolini G, Narvaiza I, Bustos M, Duarte M, Tirapu I, Bilbao R, et al. Alpha(v)beta(3) integrin-mediated adenoviral transfer of interleukin-12 at the periphery of hepatic colon cancer metastases induces VCAM-1 expression and T-cell recruitment. Mol Ther 2001;3:665–72.
50. Narazaki H, Zhu Y, Luo L, Zhu G, Chen L. CD137 agonist antibody prevents cancer recurrence: contribution of CD137 on both hematopoietic and nonhematopoietic cells. Blood 2010;115:1941–8.
51. Houot R, Goldstein MJ, Kohrt HE, Myklebust JH, Alizadeh AA, Lin JT, et al. Therapeutic effect of CD137 immunomodulation in lymphoma and its enhancement by Treg depletion. Blood 2009;114:3431–8.

Cancer Research
The Journal of Cancer Research (1916–1930) | The American Journal of Cancer (1931–1940)

AACR American Association for Cancer Research

Agonist Anti-CD137 mAb Act on Tumor Endothelial Cells to Enhance Recruitment of Activated T Lymphocytes

Asís Palazón, Alvaro Teijeira, Iván Martínez-Forero, et al.

Cancer Res 2011;71:801-811. Published OnlineFirst February 1, 2011.